Supplemental Information

Insulin Regulates Astrocyte Gliotransmission and Modulates Behavior

Weikang Cai[1], Chang Xue[2], Masaji Sakaguchi[1,3], Masahiro Konishi[1], Alireza Shirazian[4], Heather A. Ferris[1,5], Mengyao Li[1], Ruichao Yu[6], Andre Kleinridders[1,7,8], Emmanuel N. Pothos[2] and C. Ronald Kahn[1]

Supplemental Experimental Procedures

Animals. $IR^{f/f}$ mice were generated previously in the lab (1) and bred onto a C57B6/J background. GFAP-Cre mice expressing a 2.2-kb fragment of the human GFAP promoter (2) were obtained from the National Cancer Institute Mouse Repository. Astrocyte-specific IRKO mice were created by crossing $IR^{f/f}$ mice with GFAP-Cre mice (GIRKO). $IR^{f/f}$ littermates were used as controls. In addition, GIRKO mice were crossed to mice carrying a transgene for GFP under the control of human GFAP promoter (JAX 003257) to label $GFAP^{+}$ astrocytes in mice brain (GIRKO/GFP).

To delete IR in adult animals, astrocyte-specific inducible IRKO mice (iGIRKO) were generated by crossing $IR^{f/f}$ mice with GFAP-CreERT2 mice (JAX 012849). For the induction of CreERT2-mediated flox allele recombination, mice were daily injected (i.p.) with 100 mg/kg tamoxifen (Sigma) dissolved in 10% ethanol and 90% peanut oil (Sigma) for 5 days at 8 weeks of age (3). Tamoxifen was also given to $IR^{f/f}$ littermates that lack the GFAP-CreERT2 transgene to serve as controls. All the behavioral analyses of mice were conducted 6 weeks after the last injection.

Recombination efficiency for the GFAP-Cre and GFAP-CreERT2 mice was determined by crossing each Cre mouse with mTmG mice (JAX 007676). The GFP^{+} cells (flox allele recombined cells) were estimated by immunofluorescence.

Reagents and materials. AAV-DJ/8 helper-free system was purchased from Cell Biolabs. The 2.2-kb fragment of human GFAP promoter sequence was amplified from mouse tail DNA of *GFAP*-Cre mice by PCR using primer pair (forward: 5'- AAT GCT AGC CCT CCC TCT CTG TGC TGG G -3'; reverse: 5'- AAT GAA TTC GCG AGC AGC GGA GGT GAT G -3') and cloned into pscAAV empty vector. GFP and Cre:GFP fusion cDNA were subsequently cloned into pscAAV-GFAP-promoter construct generated above. A human Munc18c cDNA clone obtained from GE Lifescience was amplified by

PCR using primer pair (forward: 5'- AAT GGT ACC AAT GGC GCC GCC GG -3'; reverse: 5'- AAT GGA TCC CTA TTC ATC TTT AAT TAA GGA GAC -3') and subcloned into 3XFlag-CMV-10 empty vector (Sigma). pacAd5-Flag-Munc18c was then generated by PCR amplification and cloning of 3XFlag-hMunc18c fragment into pacAd5-CMV-IRES-GFP vector using primer pair (forward: 5'- AAT GCT TGA TAT CGA ATT ACC GTC AGA ATT AAC CAT GG -3'; reverse: 5'- AAT CGG GCT GCA GGA ATT CCC GGG ATC CCT ATT CAT CT -3') and In-Fusion HD cloning kit (Clontech).

Imipramine hydrochloride (Sigma) was dissolved in ethanol at a stock concentration of 25 mg/ml. ATP-γ-S (50 mM stock), 2-Me-SATP (100 mM stock) (Tocris), pramipexole (2 mg/ml stock) (Sigma) and 8-OH-DPAT (1 mg/ml stock) (Tocris) were dissolved in water and further diluted in aCSF or saline as indicated to working concentrations,

Rabbit anti-IGF1Rβ (#3027), rabbit anti-phospho-IR/IGF1R (#3024), rabbit anti phospho-Akt (S473) (#9271), rabbit anti-Akt (#4685), rabbit anti-phospho-GSK3α/β (S21/9) (#8566), rabbit anti-phospho-ERK1/2 (T202/Y204) (#9101), rabbit anti-ERK1/2 (#9102), and rabbit anti-c-fos (#2250) were purchased from Cell Signaling. Rabbit anti-phospho-IRS-1 (Y612) (#09-432), mouse anti-GFAP (#MAB-360), mouse anti-NeuN (#MAB-377B) and rabbit anti-VNUT (#ABN110) were from Millipore. Mouse anti-SNAP23 (#sc-166244), mouse anti-pY(20) (#sc-508), rabbit anti-IRβ (#sc-711), rabbit anti-GSK3β (#sc-9166) and HRP-conjugated β-Actin (#sc-1616-HRP) were purchased from Santa Cruz. Rabbit anti-GFAP (#ab7260), rabbit anti-GLAST (#ab416), rabbit anti-S100β (#ab53642), chicken anti-TH IgY (#ab76442), chicken anti-GFP IgY (#ab13970), Alexa488-conjugated goat anti-chicken IgY (#ab150169) were purchased from Abcam. Rabbit anti-syntaxin-4 (#PA5-22358) for immunoblotting was purchased from Thermo, while rabbit anti-syntaxin-4 (#110041) for immunoprecipitation was purchased from

Synaptic Systems. Rabbit anti-Munc18c antibody (#13764-1-AP) was purchased from ProteinTech. Mouse monoclonal anti-Flag (M2) antibody (#F1804) was from Sigma. Mouse anti-IRS-1 antibody (#611394) was from BD Biosciences. Rabbit anti-VAMP3 antibody (#NB300-510) was from Novus Biologicals. HRP-conjugated goat anti-mouse (#NA931) or rabbit IgG (#NA934) secondary antibodies were purchased from GE Healthcare. Alexa fluoro dye conjugated secondary antibodies for immunofluorescence studies were all purchased from ThermoFisher Scientific.

Mouse restraint and serum corticosterone measurement. ~30 μl blood from 6-month-old male and female mice were collected from nicked tails using capillary tubes. 15 min later, each mouse was restrained in a restraining tube (1 1/4" internal diameter by 3 1/2" length with an adjustable restraining cap and slots for air circulation) for 5 min. 15 min after restraint, another 30 μl blood was collected from each mouse. Serum was collected by centrifugation of blood samples before and after restraint (9,000 rpm, 15 min, 4°C). The content of corticosterone from mouse serum before and after restraint was measured by corticosterone ELISA kit (Enzo Lifesciences).

Stride length. Mice were first habituated to a runway (4.5 cm wide, 42 cm long with 12 cm high borders, floor covered by white chromatography paper) by three straight runs the day before the experiment. On the second day, the right front pawn of each mouse was painted with black ink, and the mouse was allowed to pass through the runway. The chromatography paper with footprints was collected after each run. The distance of the tip of the toe of the footprints from one step to the next was measured. The stride length of one mouse was determined by averaging the four longest distances measured

(corresponding to the maximal velocity) for each mouse. Runs in which the mouse made stops or obvious decelerations were excluded from the analysis and repeated.

Grip strength. Each mouse was held from the tip of its tail and the front paws grasped the grid of the Grip Strength Meter (Columbus Instruments, Columbus, OH). The grip was released when the mouse was pulled back gently. Hind limbs were kept free during the test. Each animal was tested 3 times each day with a 5 min break between each measurement. The measurements were repeated for 3 days, and the grip strength for each mouse was determined by averaging the maximal forces measured from each day.

Maximum exercise capacity by treadmill. Maximal exercise tolerance was measured in 6-month-old and 18-month-old mice using a treadmill running protocol as previously described (4). In brief, mice were given 30 minutes each to acclimate to the treadmill (Columbus Instruments, Columbus, OH) for 3 days. They then exercised with increased speed and slope of the treadmill until the mouse reached exhaustion.
Maximal exercise tolerance was determined by the cumulative amount of work (kJ) that each mouse performed, calculated as body weight (kg) X vertical distance covered (m) X 9.81.

Metabolic assessment. The body compositions of both 3-month-old GIRKO mice and $IR^{f/f}$ littermates were measured by DEXA scanning (Lunar PIXImus2 densitometer, GE Medical Systems). For metabolic assessment of mice, 3-month-old GIRKO mice and $IR^{f/f}$ littermates were housed individually in the CLAMS units (Columbus Instruments) for a 24-h acclimation, followed by 72-h measurement period. The activity, food intake, water intake, VO_2, VCO_2 and RER were determined. Lean body mass was used to normalize the raw data of VO_2 and VCO_2. Glucose tolerance tests were performed in 3-month-old

or 1-year-old overnight (16 h) fasted mice by i.p. injection of glucose (2 g/kg body weight). Blood glucose was measured at 15, 30, 60 and 120 min post injection. Insulin tolerance tests were performed in mice by i.p. injection of insulin (1 mU/kg body weight for male mice and 1-year-old male and female mice, and 0.5 mU/kg body weight for 3-month-old female mice) following a 4 h fast early in the morning. Blood glucose was measured at 15, 30, 60 and 90 min post injection.

Insulin ELISA. Insulin levels in mouse sera were quantified using a commercially available insulin ELISA kit (Crystal Chem) according to the manufacturer's manual.

Adenovirus-associated virus (AAV-DJ/8) production. The production of AAV-DJ/8-GFAP-Cre:GFP and AAV-DJ/8-GFAP-GFP was according to the manual of AAV Helper Free System from Cell Biolabs. Briefly, 293AAV cells (Cell Biolabs) maintained in DMEM + 10% FBS were co-transfected with pscAAV-GFAP-Cre:GFP or GFP only, pAAV-DJ/8 and pHelper plasmids at 1:1:1 ratio using 1 mg/ml PEI reagent. 3 days after transfection, cells were collected, washed with sterile PBS and pelleted by centrifugation.

AAV viral particles were purified using AAVpro Purification kit (Takara) following the manufacturer's manual. The final titer of the purified viral particles was determined by qPCR using primer pairs for GFP (forward: 5'- GAC AAC CAC TAC CTG AGC AC -3'; reverse: 5'- CAG GAC CAT GTG ATC GCG -3') and Cre (forward: 5'- TGA CGG TGG GAG AAT GTT AAT C-3'; reverse: 5'- GCT ACA CCA GAG ACG GAA ATC-3'). The pscAAV-hGFAP-Cre:GFP and pscAAV-hGFAP-GFP plasmids were used to setup the standard.

Adenovirus preparation, amplification and infection on primary astrocytes. The package and amplification of adenovirus encoding Cre:GFP, GFP or Flag-hMunc18c

were conducted using RAPAd CMV Adenoviral Bicistronic Expression System (Cell Biolabs) following manufacturer's manual. The adenoviral particles were purified using Adeno-X Maxi Purification kit (Clontech) following manufacturer's manual. The titer of the purified adenovirus was determined by UV absorbance. Primary astrocytes were infected with adenovirus (1 X 10^9 GC/ml) for 24 h and cultured for an additional 5 days before experiments.

Insulin signaling on cultured astrocytes. Primary astrocytes were serum starved for 5 h with DMEM containing 0.1% BSA, and stimulated with 1 or 10 nM insulin for 15 min. After stimulation, cells were washed immediately with ice-cold PBS once before lysis and scraped down in RIPA lysis buffer complemented with 50 mM KF, 50 mM β-glycerolphosphate, 2 mM EGTA (pH 8), 1 mM Na_3VO_4 and 1X protease inhibitor cocktail (Calbiochem). Protein concentrations were determined using the Pierce 660 nm Protein Assay Reagent (Bio-Rad). Lysates (10–20 μg) were resolved on SDS-PAGE gels, transferred to PVDF membrane for immunoblotting.

Co-immunoprecipitation. To examine syntaxin-4 and VAMP3 interaction in response to insulin, control and IRKO astrocytes were serum starved in DMEM + 0.1% BSA for 5 h, followed by 100 nM insulin stimulation for 30 min. After stimulation, cells were washed immediately with ice-cold PBS once and lysed in lysis buffer [20 mM Hepes (pH 7.4), 150 mM NaCl, 50 mM KF, 50 mM β-glycerolphosphate, 2 mM EGTA (pH 8), 1 mM Na_3VO_4, 1% Triton X-100, 10% glycerol and 1X protease inhibitor cocktail (Calbiochem)]. Protein concentrations were determined using the Pierce 660 nm Protein Assay Reagent (Bio-Rad). To immunoprecipitate syntaxin-4 containing complex, 800 μg protein lysates were incubated with 1 μg anti-syntaxin-4 antibody

(Synaptic Systems) in a total volume of 800 μl overnight at 4°C with end-to-end rotation. The immunocomplexes were incubated with 20 μl protein A/G-conjugated magnetic beads for 1 h at 4°C with end-to-end rotation. The immunocomplexes were then pulled down with magnetic rack and washed sequentially: 1 time with lysis buffer, two times with lysis buffer + 500 mM NaCl, and two times with lysis buffer. Bound proteins were eluted by incubation for 5 min at 100°C in 1 X SDS loading buffer. The bound proteins along with 10 μg total cell lysates from each sample were resolved using SDS-PAGE, transferred to PVDF membranes and subjected to immunoblotting using the indicated antibodies.

Immunoblotting. PVDF membranes were blocked in Starting Block T20 (ThermoFisher) at room temperature for 1 h, incubated with the indicated primary antibody in Starting Block T20 solution overnight at 4°C. Membranes were washed three times with 1X PBST, incubated with HRP-conjugated secondary antibody (GE Healthcare, anti-mouse IgG, NA931; anti-rabbit IgG, NA934; 1:20,000) in Starting Block T20 for 1 h and signals detected using Immobilon Western Chemiluminescent HRP Substrate (Millipore).

Tissue section preparation. Mice were anesthetized with an intraperitoneal (i.p.) injection of Avertin (300 mg/kg), transcardially perfused with heparinized saline followed by 10% buffered formalin, and decapitated. After 24 h of post-fixation in 10% buffered formalin, brains were removed from the skull, post-fixed for an additional 24 h, cryoprotected in 30% sucrose, and quickly frozen on dry ice. Serial coronal 30 μm sections were cut using a freezing Cryostat station for further immunohistochemical analysis.

Immunofluorescence. Brain sections were placed in 24-well plates and washed three times in 1X PBS for 5 min. The sections were then permeabilized and blocked by the addition of 5% normal goat serum (NGS) and 0.1% Triton X-100 in 1X PBS and agitated for 30 min at RT. After blocking, primary antibodies diluted in 1X PBS containing 1% NGS + 0.1% Triton X-100 were added with gentle rocking overnight at 4°C. On the following day, sections were washed four times with 1X PBST and secondary antibody diluted in 1X PBS containing 1% NGS + 0.1% Triton X-100 was applied. Sections were then washed four times with 1X PBST and coverslipped with SlowFade Gold containing DAPI (Invitrogen). Confocal images were taken using confocal microscopy (Zeiss 710). The mean intensity and pixel areas were analyzed using Image J software.

Quantification of c-fos+ neurons in nucleus accumbens. $IR^{f/f}$ and iGIRKO mice at basal condition or 1 h post FST were sacrificed and their brains collected, fixed in 10% formalin, and subjected to sucrose processing and cryosectioning as described above. The brain sections were co-stained for c-fos and NeuN. Multiple confocal images were taken in the area of nucleus accumbens for each mouse (4 images per mouse, 2 from each hemisphere) using 20X objective. Total number of $c\text{-}fos^{+}/NeuN^{+}$ cells and $NeuN^{+}$ cells were counted using ImageJ and presented as percentage of $c\text{-}fos^{+}NeuN^{+}$ / total $NeuN^{+}$ cells.

Isolation of GFP^{+} astrocytes using fluorescence-activated cell sorting (FACS). Brains from 4-week-old $IR^{f/f}$/GFP or GIRKO/GFP mice were extracted, minced and further dissociated using 1 X Accutase (ThermoFisher) supplemented with 80 U/ml DNase I (Sigma) at 37°C for 20 min, followed by gentle trituration in Hybernate A media (Invitrogen) plus 1% FBS. Cell suspension was passed through a 70 μm filter, overlayed

on top of isotonic percoll gradient (top phase: 11%, 3 ml; bottom phase: 30%, 2 ml) and centrifuged 400X g, 5 min 4 °C. Dissociated astrocytes were retrieved using a 25-gauge needle from the interface between 11% and 13% phases and pelleted by centrifugation. The cell pellet was resuspended in 500 μl 1X PBS + 5% FBS + 1.5 μM propidium iodide and subjected to FACSAria cell sorter for analysis. GFP^+ from both CTR/GFP and GIRKO/GFP mice were sorted and used for total RNA extraction and gene expression analysis.

Total RNA isolation, RT-PCR and quantitative real-time PCR. Total RNA was extracted using an RNeasy mini kit (Qiagen) following manufacturer's manual from either primary astrocytes or mouse brain tissues. To generate cDNA libraries from isolated total RNA samples, 1 μg of RNA was reverse transcribed using a High Capacity cDNA Reverse Transcription kit (Applied Biosystems) according to the manufacturer's instructions. Quantitative real time PCR was performed using the SYBR Green PCR master mix (Bio-Rad). Fluorescence was monitored and analyzed in an ABI Prism 7900 HT sequence detection system (Applied Biosystems). TBP expression was used to normalize gene expression. Amplification of specific transcripts was confirmed by analyzing melting curve profiles at the end of each PCR. All the primer sequences used for this study were listed in Supplemental Table 1.

Reference

1. Bruning JC, Michael MD, Winnay JN, Hayashi T, Horsch D, Accili D, Goodyear LJ, and Kahn CR. A muscle-specific insulin receptor knockout exhibits features of the metabolic syndrome of NIDDM without altering glucose tolerance. *Mol Cell.* 1998;2(5):559-69.

2. Bajenaru ML, Zhu Y, Hedrick NM, Donahoe J, Parada LF, and Gutmann DH. Astrocyte-specific inactivation of the neurofibromatosis 1 gene (NF1) is insufficient for astrocytoma formation. *MolCell Biol.* 2002;22(14):5100-13.

3. Sakaguchi M, Fujisaka S, Cai W, Winnay JN, Konishi M, O'Neill BT, Li M, Garcia-Martin R, Takahashi H, Hu J, et al. Adipocyte Dynamics and Reversible Metabolic Syndrome in Mice with an Inducible Adipocyte-Specific Deletion of the Insulin Receptor. *Cell Metab.* 2017;25(2):448-62.

4. Li M, Vienberg SG, Bezy O, O'Neill BT, and Kahn CR. Role of PKCdelta in Insulin Sensitivity and Skeletal Muscle Metabolism. *Diabetes.* 2015;64(12):4023-32.

Supplemental Figure 1

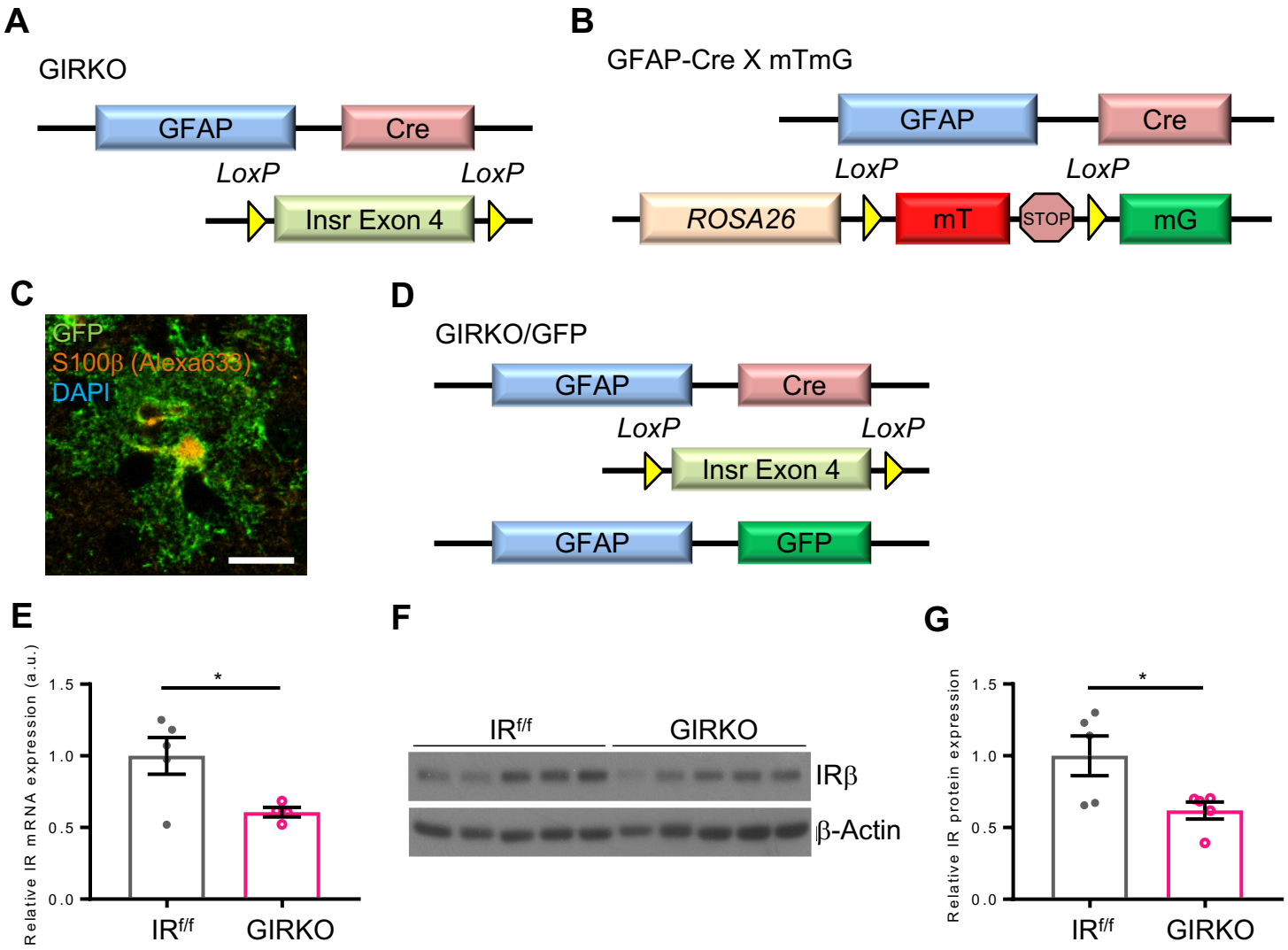

Supplemental Figure 1. Generation of mice lacking insulin receptors in astrocytes. (A) The schematics of strategy to generate astrocyte specific insulin receptor knockout mice by crossing the $IR^{f/f}$ mice with the mice containing human GFAP-promoter-driven Cre. **(B)** The schematics of strategy to generate GFAP-Cre X mTmG lineage tracing mice to confirm the Cre-dependent recombination in astrocytes. **(C)** Co-immunostaining of GFP and astrocyte-specific marker S100β in nucleus accumbens from GFAP-Cre X mTmG mouse, indicating specific flox allele recombination in astrocyte in nucleus accumbens. Scale bar: 20 μm. **(D)** The schematics of strategy to generate astrocyte specific GFP reporter mice with or without insulin receptor deletion in astrocytes, which allow the labeling of $GFAP^+$ astrocytes with GFP. **(E)** Relative expression of insulin receptor mRNA in the nucleus accmbens (NAc) of 3-month-old female $IR^{f/f}$ and GIRKO mice. TBP was used as housekeeping gene. *, $P < 0.05$, two-tailed Student's *t*-test, $n=5$ for $IR^{f/f}$, $n=4$ for GIRKO. **(F)** Immunoblotting of insulin receptor-beta subunit in the nucleus accmbens (NAc) of 3-month-old female $IR^{f/f}$ and GIRKO mice. **(G)** Densitometric analysis of relative expression of IRβ normalized to β-Actin in the nucleus accmbens (NAc) of 3-month-old female $IR^{f/f}$ and GIRKO mice. *, $P < 0.05$, two-tailed Student's *t*-test, $n=5$. All data are presented as mean ± SEM.

Supplemental Figure 2 Male mice

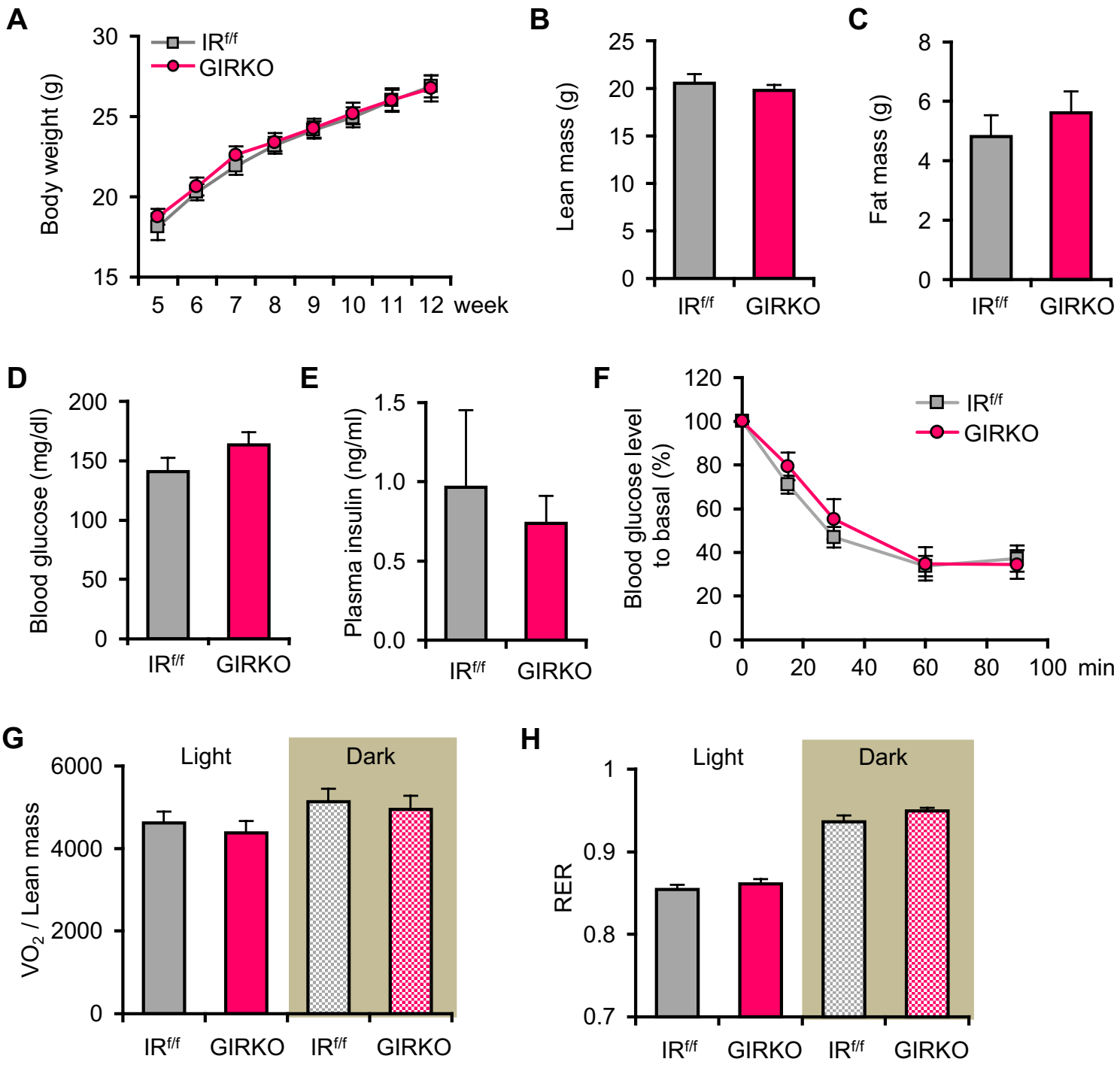

Supplemental Figure 2. Metabolic assessment of male GIRKO mice. (A) The body weight of male $IR^{f/f}$ and GIRKO mice from 5 weeks of age to 12 weeks of age. *n*=24 for $IR^{f/f}$, *n*=18 for GIRKO. **(B)** Lean body mass of 3-month-old male $IR^{f/f}$ and GIRKO mice. *n*=6. **(C)** Fat mass of 3-month-old male $IR^{f/f}$ and GIRKO mice. *n*=6. **(D)** Blood glucose levels of 3-month-old male $IR^{f/f}$ and GIRKO mice under fed condition. *n*=6. **(E)** Plasma insulin levels of 3-month-old male $IR^{f/f}$ and GIRKO mice under fed condition. *n*=5 for $IR^{f/f}$, *n*=6 for GIRKO. **(F)** Insulin tolerance tests on 3-month-old male $IR^{f/f}$ and GIRKO mice by i.p. insulin (1 mU/kg) injection. *n*=8 for $IR^{f/f}$, *n*=6 for GIRKO. **(G)** Oxygen consumption of 3-month-old male $IR^{f/f}$ and GIRKO mice under light and dark cycles. The raw VO_2 data were normalized by the lean mass of each mouse. *n*=6. **(H)** Respiratory exchange ratio of 3-month-old male $IR^{f/f}$ and GIRKO mice under light and dark cycles. *n*=6. All data are presented as mean ± SEM.

Supplemental Figure 3 Female mice

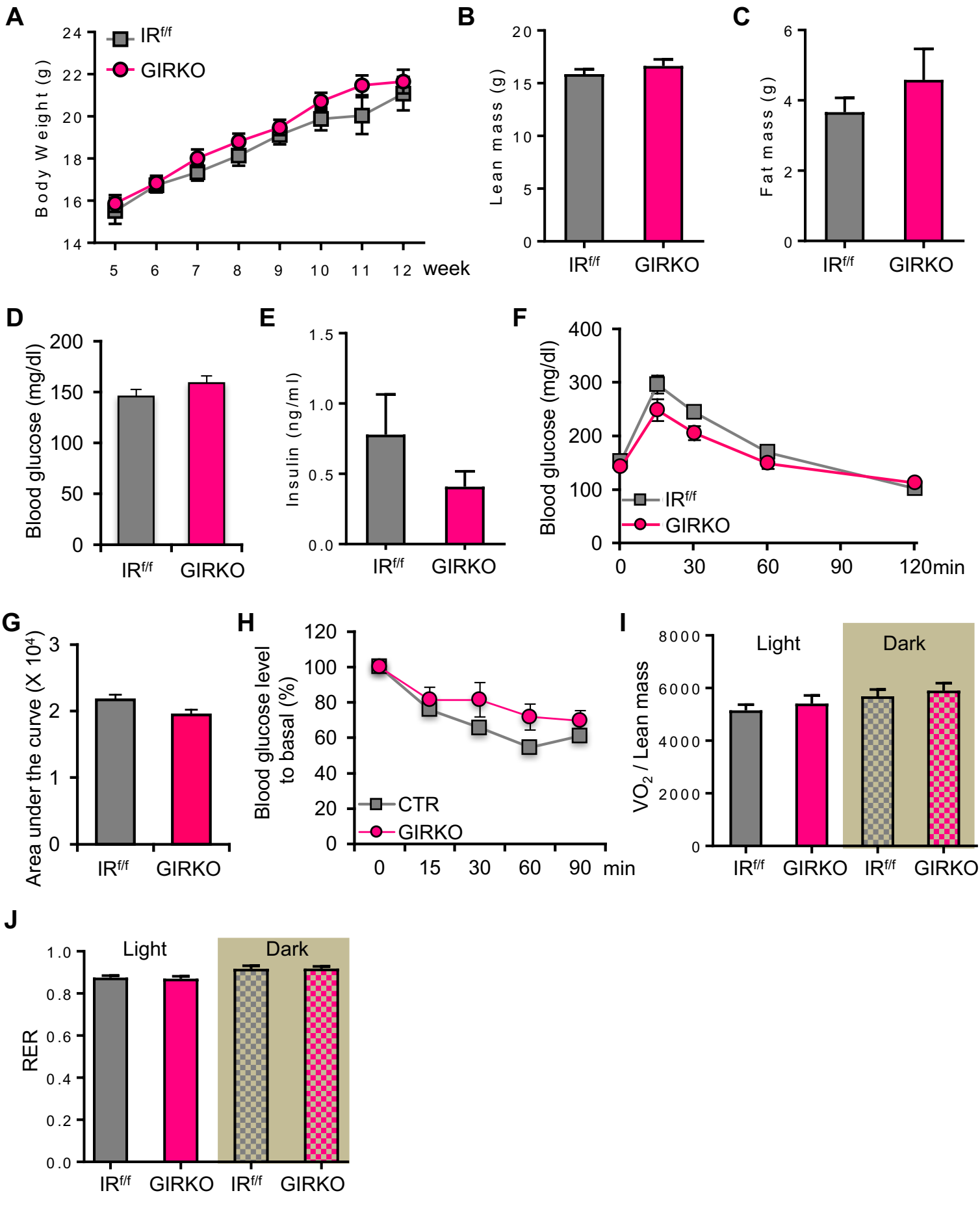

Supplemental Figure 3. Metabolic assessment of female GIRKO mice. (A) The body weight of female $IR^{f/f}$ and GIRKO mice from 5 weeks of age to 12 weeks of age. *n*=24 for $IR^{f/f}$, *n*=18 for GIRKO. **(B)** Lean body mass of 3-month-old female $IR^{f/f}$ and GIRKO mice. *n*=6. **(C)** Fat mass of 3-month-old female $IR^{f/f}$ and GIRKO mice. *n*=6. **(D)** Blood glucose levels of 3-month-old male $IR^{f/f}$ and GIRKO mice under fed condition. *n*=6. **(E)** Plasma insulin levels of 3-month-old female $IR^{f/f}$ and GIRKO mice under fed condition. *n*=5 for $IR^{f/f}$, *n*=6 for GIRKO. **(F)** Glucose tolerance tests on 3-month-old female $IR^{f/f}$ and GIRKO mice by i.p. glucose (2 g/kg) injection. *n*=7 for $IR^{f/f}$, *n*=6 for GIRKO. **(G)** Area under the curve of GTT. *n*=7 for $IR^{f/f}$, *n*=6 for GIRKO. **(H)** Insulin tolerance tests on 3-month-old female $IR^{f/f}$ and GIRKO mice by i.p. insulin (0.5 mU/kg) injection. *n*=6 for $IR^{f/f}$, *n*=6 for GIRKO. **(I)** Oxygen consumption of 3-month-old female $IR^{f/f}$ and GIRKO mice under light and dark cycles. The raw VO_2 data were normalized by the lean mass of each mouse. *n*=6. **(J)** Respiratory exchange ratio of 3-month-old female $IR^{f/f}$ and GIRKO mice under light and dark cycles. *n*=6. All data are presented as mean ± SEM.

Supplemental Figure 4 1-year-old male and female mice

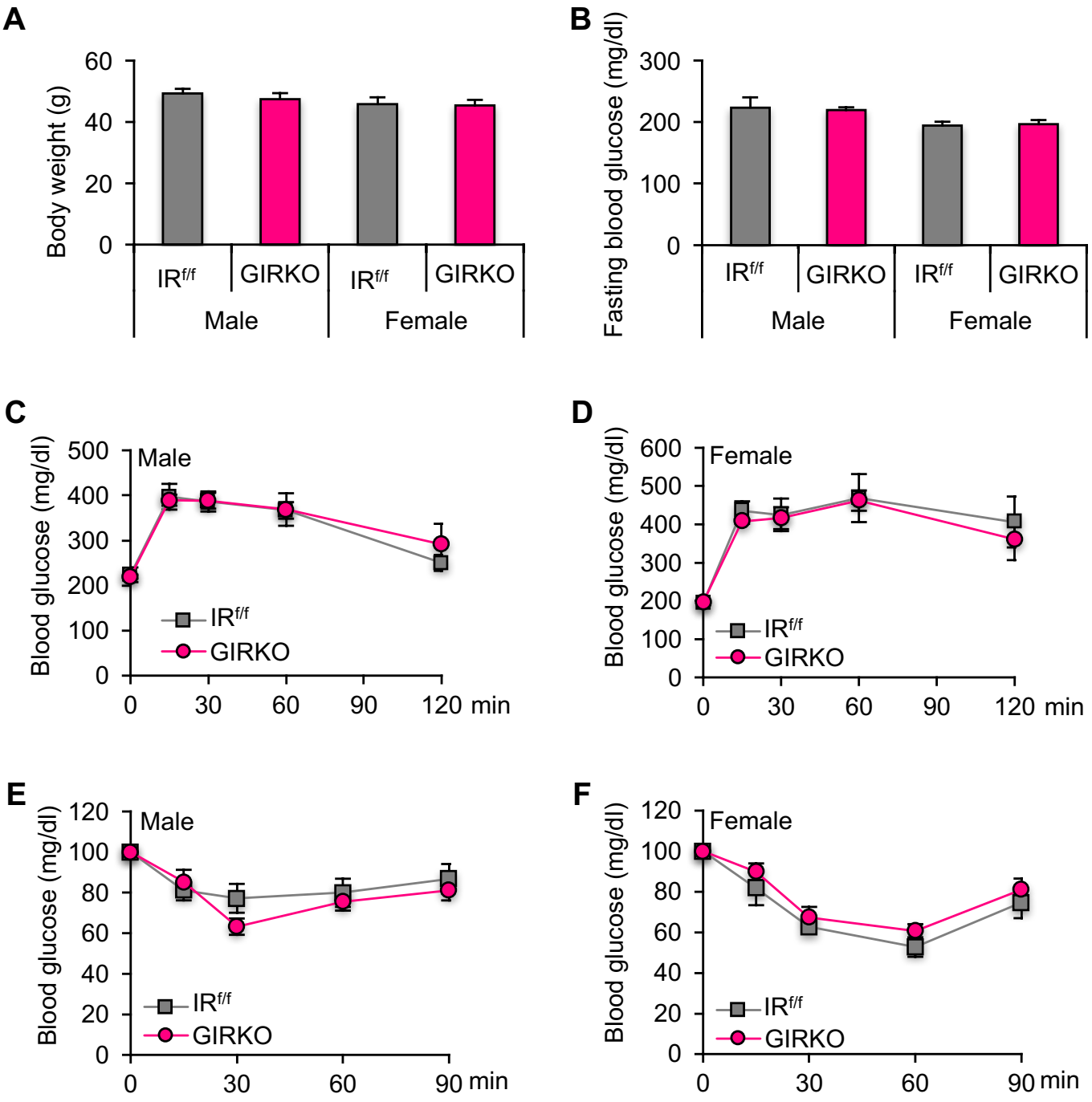

Supplemental Figure 4. Metabolic assessment of 1-year-old GIRKO mice. (A) The body weight of female IR$^{f/f}$ and GIRKO mice at 1 year of age. *n*=6 for male, *n*=7 for female. **(B)** Fasting blood glucose levels of 1-year-old male IR$^{f/f}$ and GIRKO mice after overnight fasting. *n*=6 for male, *n*=7 for female. **(C)** Glucose tolerance tests on 1-year-old male IR$^{f/f}$ and GIRKO mice by i.p. glucose (2 g/kg) injection. *n*=6. **(D)** Glucose tolerance tests on 1-year-old female IR$^{f/f}$ and GIRKO mice by i.p. glucose (2 g/kg) injection. *n*=7. **(E)** Insulin tolerance tests on 1-year-old male IR$^{f/f}$ and GIRKO mice by i.p. insulin (1 mU/kg) injection. *n*=7. **(F)** Insulin tolerance tests on 1-year-old female IR$^{f/f}$ and GIRKO mice by i.p. insulin (1 mU/kg) injection. *n*=7. All data are presented as mean ± SEM.

Supplemental Figure 5

Female mice

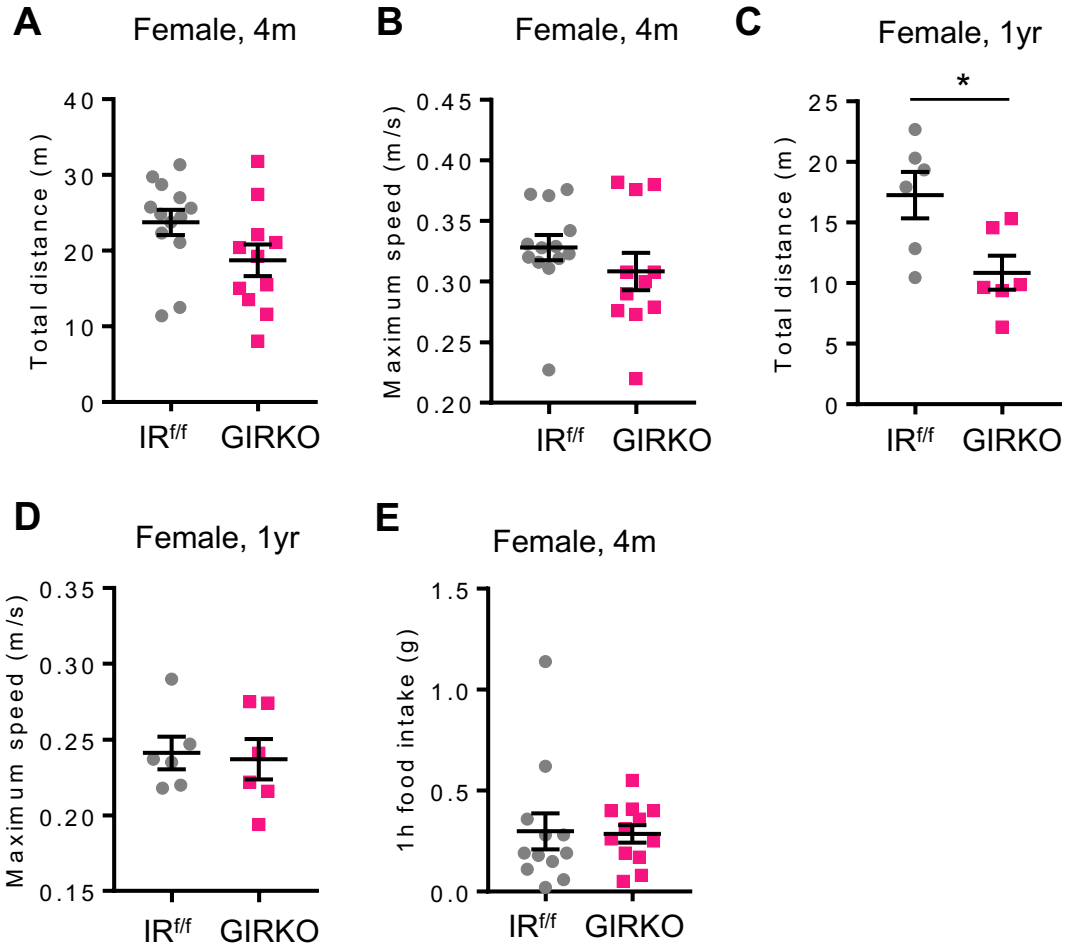

Supplemental Figure 5. Behavioral assessment of female GIRKO mice. (A) Total distance traveled by 4-month-old female IR$^{f/f}$ and GIRKO mice in open field test. *n*=13 for IR$^{f/f}$, *n*=11 for GIRKO. **(B)** Maximum speed of 4-month-old female IR$^{f/f}$ and GIRKO mice during the open field test. *n*=13 for IR$^{f/f}$, *n*=11 for GIRKO. **(C)** Total distance traveled by 1-year-old female IR$^{f/f}$ and GIRKO mice in open field test. *, $P < 0.05$, two-tailed Student's *t*-test, *n*=6. **(D)** Maximum speed of 1-year-old female IR$^{f/f}$ and GIRKO mice during the open field test. *n*=6. **(E)** One-hour food intake of 4-month-old female IR$^{f/f}$ and GIRKO mice in a housing cage immediately after the novelty suppressed feeding test. *n* =12. All data are presented as mean ± SEM.

Supplemental Figure 6 Male mice

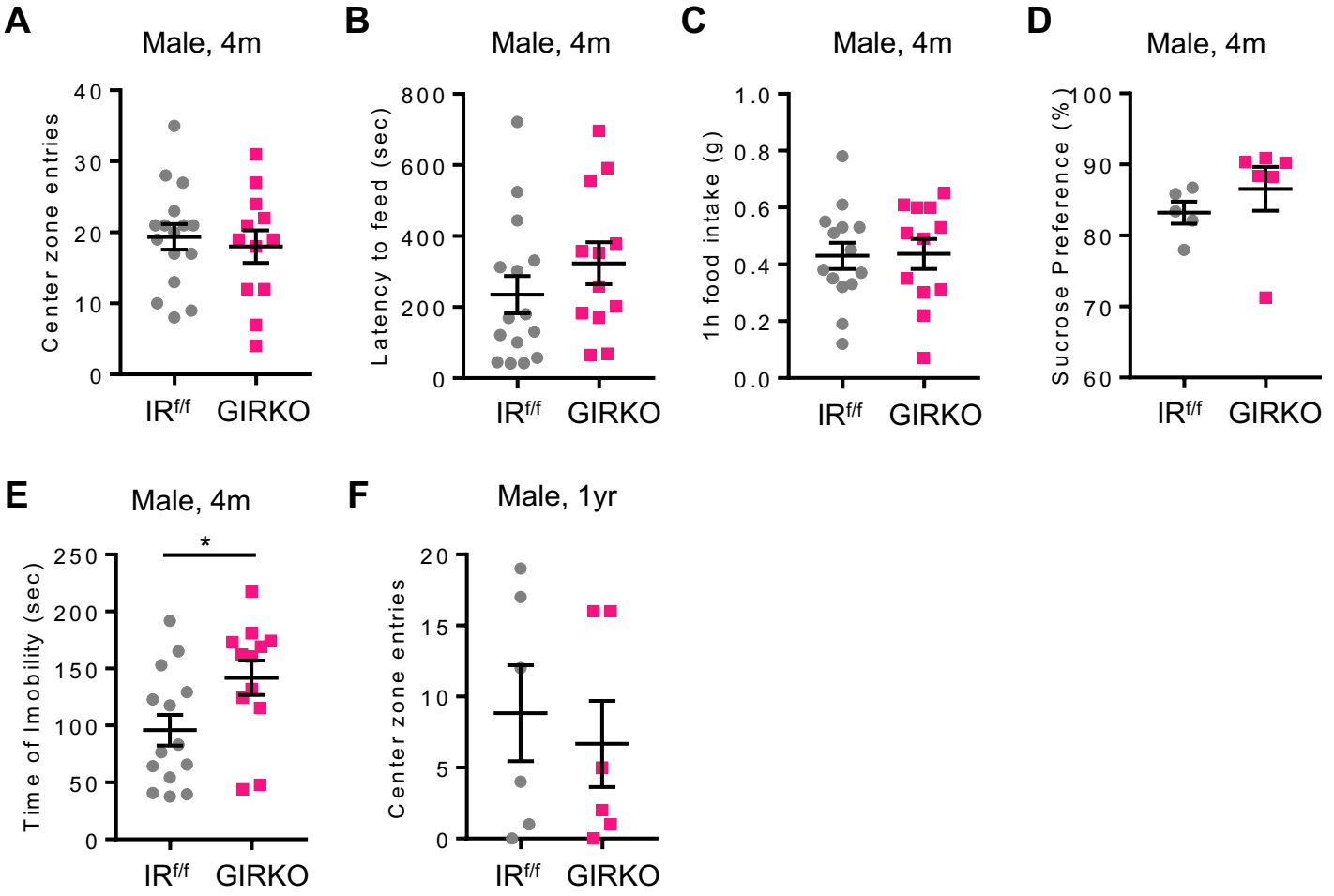

Supplemental Figure 6. Behavioral assessment of male GIRKO mice. (A) Number of center zone entries of 4-month-old male IR$^{f/f}$ and GIRKO mice in open field test. *n*=16 for IR$^{f/f}$, *n*=12 for GIRKO. **(B)** Latency to feeding of 4-month-old male IR$^{f/f}$ and GIRKO mice in novelty suppressed feeding test. *n*=15 for IR$^{f/f}$, *n*=12 for GIRKO. **(C)** One-hour food intake of 4-month-old male IR$^{f/f}$ and GIRKO mice in a housing cage immediately after the novelty suppressed feeding test. *n*=15 for IR$^{f/f}$, *n*=12 for GIRKO. **(D)** Sucrose preference of 4-month-old male IR$^{f/f}$ and GIRKO mice. *n*=5 for IR$^{f/f}$, *n*=6 for GIRKO. **(E)** Immobility time of 4-month-old male IR$^{f/f}$ and GIRKO mice during the forced swimming test. *n*=14 for IR$^{f/f}$, *n*=12 for GIRKO. **(F)** Number of center zone entries of 1-year-old male IR$^{f/f}$ and GIRKO mice in open field test. *n*=6. All data are presented as mean ± SEM.

Supplemental Figure 7

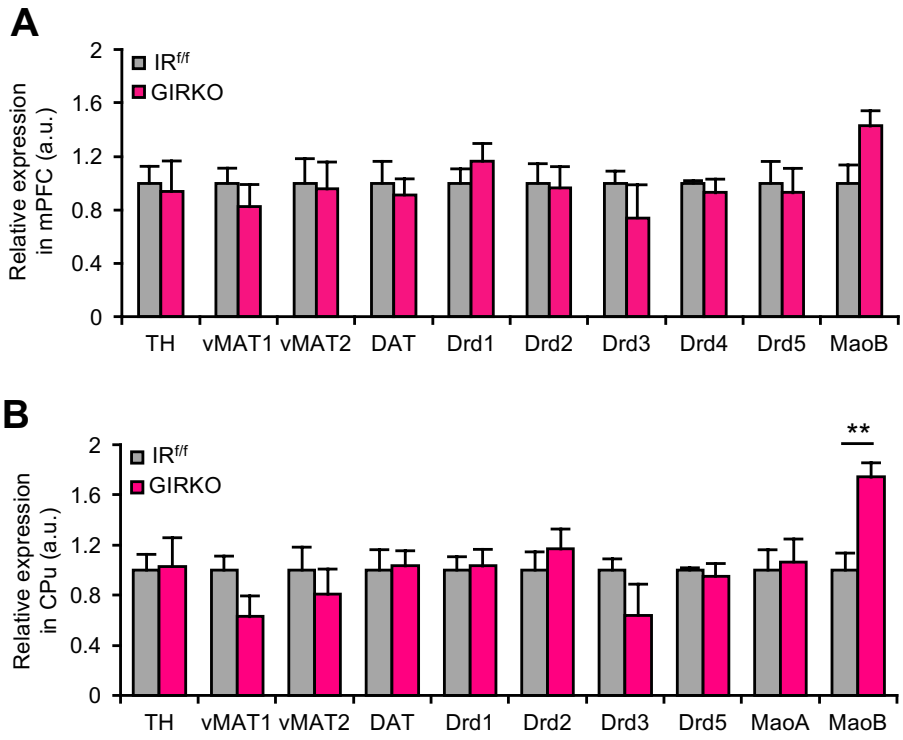

Supplemental Figure 7. Gene expression of dopamine system in the medial prefrontal cortex and caudate putamen of GIRKO mice. (A) Relative expression of enzymes and proteins involved in dopamine synthesis, vesicle loading, uptake and degradation in the medial frontal cortex (mPFC) of $IR^{f/f}$ and GIRKO mice. $n = 6$. **(B)** Relative expression of enzymes and proteins involved in dopamine synthesis, vesicle loading, uptake and degradation in the dorsal caudate putamen (CPu) of $IR^{f/f}$ and GIRKO mice. **, $P < 0.01$, $n = 6$ (two-tailed Student's *t*-test). TBP was used as housekeeping gene. All the data are presented as mean ± SEM.

Supplemental Figure 8

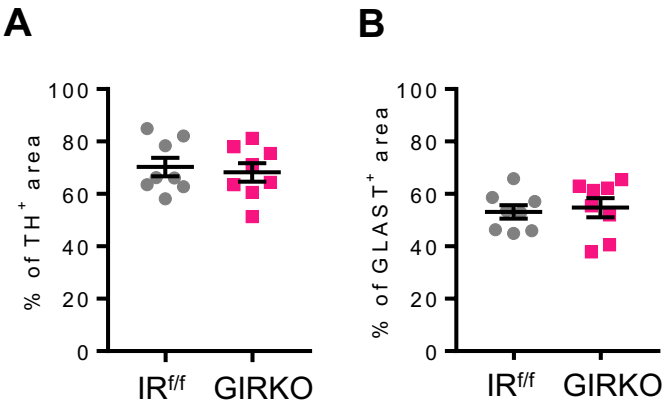

Supplemental Figure 8. The coverage areas of the dopaminergic neural fibers and astrocytes in the nucleus accumbens. (A) Percentage of TH^+ fiber area in the nucleus accumbens of $IR^{f/f}$ and GIRKO brain sections. *n*=8 random fields in nucleus accumbens from 4 mice. **(B)** Percentage of $GLAST^+$ area in the nucleus accumbens of $IR^{f/f}$ and GIRKO brain sections. *n*=8 random fields in nucleus accumbens from 4 mice. All data are presented as mean ± SEM.

Supplemental Figure 9

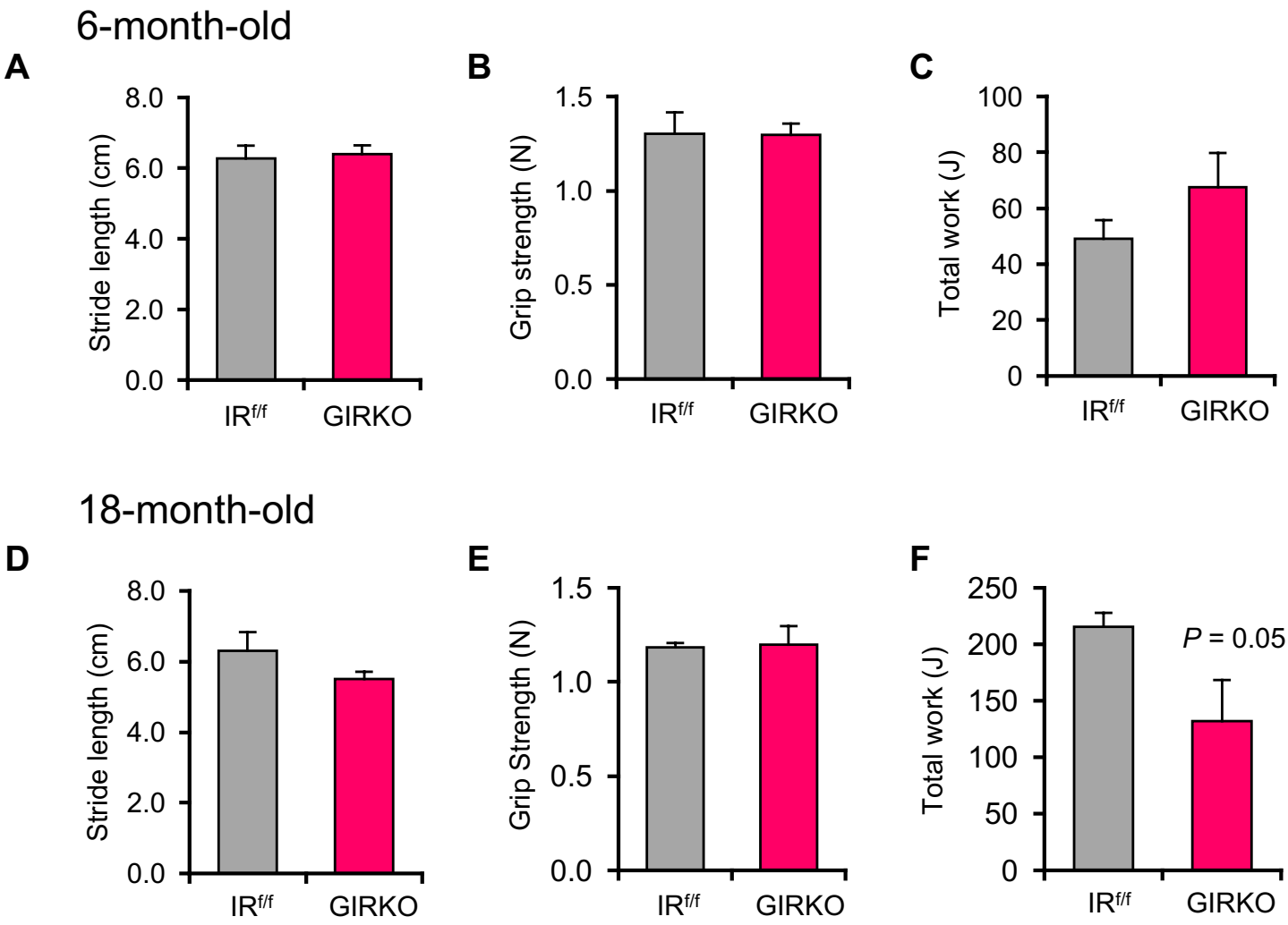

Supplemental Figure 9. Motor function analysis of young and aged female GIRKO mice. (A and D) The average stride length, **(B and E)** grip strength, and **(C and F)** total work on treadmill before exhaustion of young (6-month-old) and aged (18-month-old) female $IR^{f/f}$ and GIRKO mice. *n*=6-8 for young mice, *n*=5 for aged $IR^{f/f}$, *n*=4 for aged GIRKO.

Supplemental Figure 10

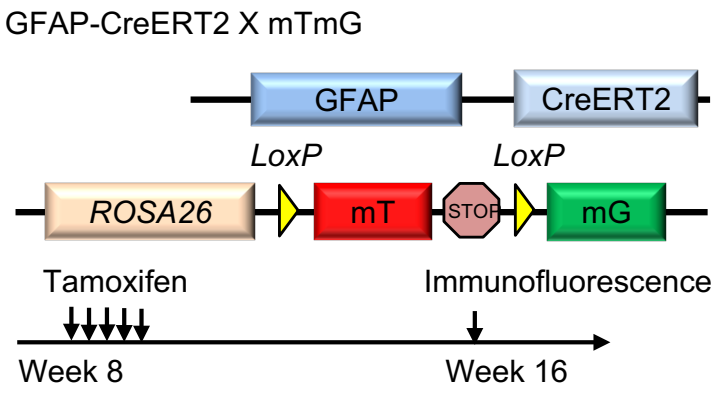

Supplemental Figure 10. Generation of inducible astrocyte-specific mTmG reporter mouse model. The schematics of strategy to generate GFAP-CreERT2 X mTmG lineage tracing mice to confirm the Cre-dependent recombination in astrocytes. To induce recombination in astrocytes, mice were injected with tamoxifen (100 mg/kg, *i.p.*) for 5 consecutive days at the age of 8 weeks. All the experiments were performed 8 weeks after the initial tamoxifen injection.

Supplemental Figure 11

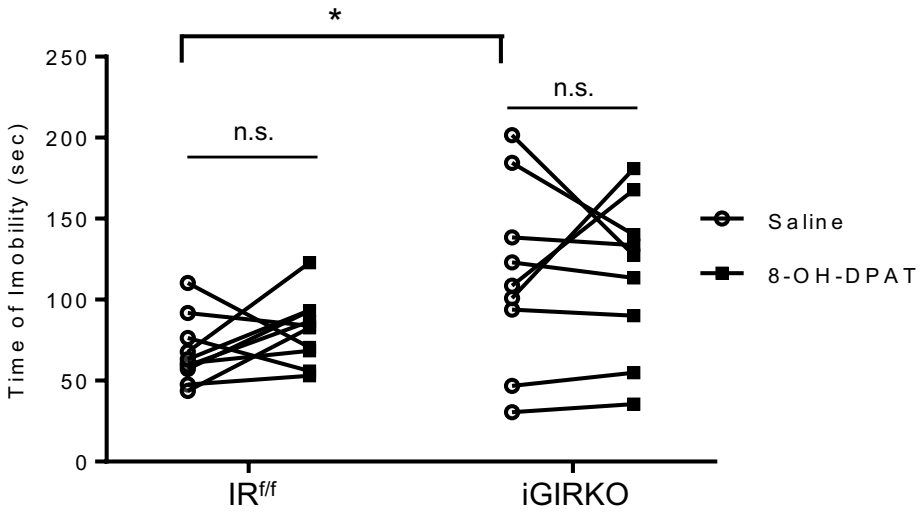

Supplemental Figure 11. Serotonin 1A receptor (5-HT1A) agonist 8-OH-DPAT has no effect on the depressive-like behavior in iGIRKO mice. Time of immobility of 4-month-old female $IR^{f/f}$ and iGIRKO mice in forced swimming test with *i.p.* injection of saline or 8-OH-DPAT (0.3 mg/kg) 1 h prior to the test. *, $P < 0.05$, repeated two-way ANOVA followed by Sidak's multiple comparisons, n=10 for $IR^{f/f}$ groups, n=9 for iGIRKO groups. Note, all the mice were injected with saline or 8-OH-DPAT *i.p.* in a randomized fashion 1 h prior to the forced swimming test. One group of mice were administrated saline followed by forced swimming test at week 1 and then administrated 8-OH-DPAT followed by forced swimming test at week 2. In the second group of mice the order of tests was reversed.

Supplemental Figure 12

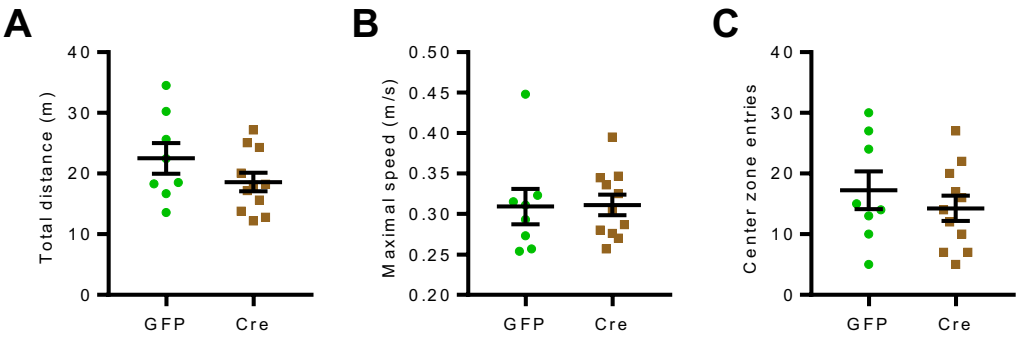

Supplemental Figure 12. Loss of IR in astrocytes in nucleus accumbens has no effect on center zone exploration and locomotive activity in open field test. (A) Total distance traveled by 4-month-old female $IR^{f/f}$ mice injected with AAV-GFAP-Cre or AAV-GFAP-GFP at nucleus accumbens in open field test. *n*=8 for GFP, *n*=11 for Cre. **(B)** Maximum speed of 4-month-old female $IR^{f/f}$ mice injected with AAV-GFAP-Cre or AAV-GFAP-GFP at nucleus accumbens during the open field test. *n*=8 for GFP, *n*=11 for Cre. **(C)** Number of center zone entries of 4-month-old female $IR^{f/f}$ mice injected with AAV-GFAP-Cre or AAV-GFAP-GFP at nucleus accumbens in open field test. *n*=8 for GFP, *n*=11 for Cre. All data are mean ± SEM.

Supplemental Figure 13

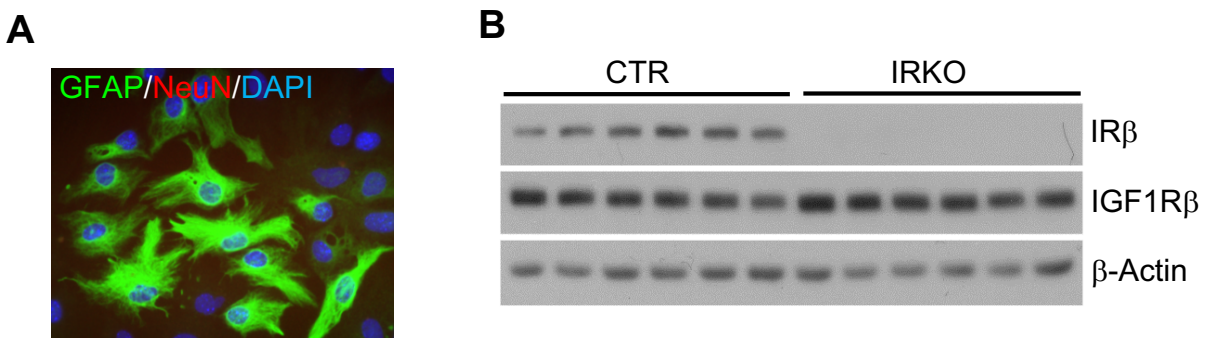

Supplemental Figure 13. Generation of IR-deficient primary astrocytes. (A) Representative images of primary astrocyte culture co-stained with GFAP/NeuN/DAPI. **(B)** Western blotting showing the specific deletion of insulin receptor, but not IGF-1 receptor, in astrocytes.

Supplemental Figure 14

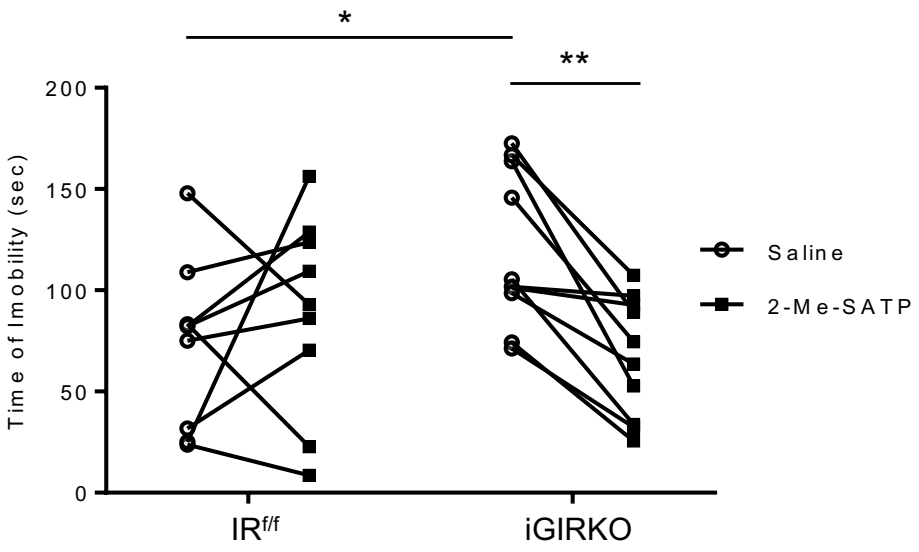

Supplemental Figure 14. Purinergic receptor agonist 2-Me-SATP infusion into the intracerebral ventricle rescued the depressive-like behavior in iGIRKO mice. Time of immobility of 4-month-old female $IR^{f/f}$ and iGIRKO mice in forced swimming test with *i.c.v.* infusion of saline or 20 pmol 2-Me-SATP 1 h prior to the test. *, $P < 0.05$, **, $P < 0.01$, repeated two-way ANOVA followed by Sidak's multiple comparisons, $n=9$ for $IR^{f/f}$ groups, $n=10$ for iGIRKO groups. Note, all the mice were injected with 2 μl saline or 2-Me-SATP (10 mM) *i.c.v.* in a randomized fashion 1 h prior to the forced swimming test. One group of mice were administrated saline followed by forced swimming test at week 1 and then administrated 2-Me-SATP followed by forced swimming test at week 2. In the second group of mice the order of tests was reversed.

Supplemental Figure 15

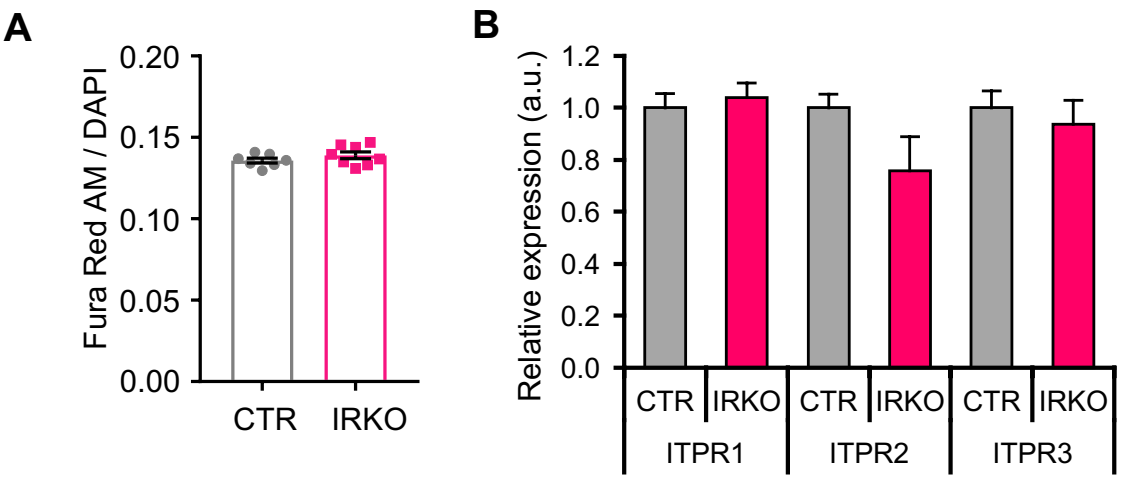

Supplemental Figure 15. Exocytosis machinery in IRKO astrocytes. (A) Intracellular [$Ca2^{+}$] levels of CTR and IRKO astrocytes measured by calcium indicator Fura Red AM and normalized by DAPI. **(B)** Relative expression of IP3 receptors in CTR and IRKO astrocytes. TBP was used as housekeeping gene. *n*=6. All data are presented as mean ± SEM.

Supplemental Table 1

Primer list for quantitative real-time PCR

Gene Symbol	Primer direction	Primer sequence
TBP	Forward	ACCCTTCACCAATGACTCCTATG
TBP	Reverse	TGACTGCAGCAAATCGCTTGG
IR	Forward	AAATGCAGGAACTCTCGGAAGCCT
IR	Reverse	ACCTTCGAGGATTTGGCAGACCTT
IGF1R	Forward	ATCGCGATTTCTGCGCCAACA
IGF1R	Reverse	TTCTTCTCTTCATCGCCGCAGACT
TH	Forward	AAGATCAAACCTACCAGCCG
TH	Reverse	TACGGGTCAAACTTCACAGAG
vMAT1	Forward	GGCCAGTGTCTATACGGATAAC
vMAT1	Reverse	ATGAGGAATGGTGAGGACTTG
vMAT2	Forward	ATCCTGTTCATCGTGTTCCTC
vMAT2	Reverse	GGCAGTCTGGATTTCCGTAG
DAT	Forward	TGGCACATCTATCCTCTTTGG
DAT	Reverse	GACCACGACCACATACAGAAG
Drd1	Forward	AGCGTAGTCTCCCAGATCG
Drd1	Reverse	GCCTCTTCCTGGTCAATCTC
Drd2	Forward	ACCACTCAAGGGCAACTG
Drd2	Reverse	TGACAGCATCTCCATTTCCAG
Drd3	Forward	TTCACTATCAGCATGGCACC
Drd3	Reverse	GGTTGGAGATGGAGCAGATG
Drd5	Forward	AAAATCTCACCACTCACCCC
Drd5	Reverse	AAGCATAAGCACACCAGGAG
MaoA	Forward	TGGTTCTTGTGGTATGTGAGG
MaoA	Reverse	AGCTTCACTTTATCCCCAAGG
MaoB	Forward	GCCCGTCCATTATGAAGAGAAG
MaoB	Reverse	CTGTTTCAGTGCCTGCAAAG
GFAP	Forward	GAAAACCGCATCACCATTCC
GFAP	Reverse	CTTAATGACCTCACCATCCCG
Aqp4	Forward	TATCCAGTGGTTTGCCCAGT
Aqp4	Reverse	GCAATTGGACATTTGTTTGC
Aldoc	Forward	TGGTTAGGAGAGGAAGTAGAAGG
Aldoc	Reverse	CGATCCGTAGAGCAATATCCG
GS	Forward	TGAACAAAGGCATCAAGCAAATG
GS	Reverse	CAGTCCAGGGTACGGGTCTT
GLT-1	Forward	TAACTCTGGCGGCCAATGGAAAGT
GLT-1	Reverse	ACGCTGGGGAGTTTATTCAAGAAT
GLAST	Forward	CCCATCCCAGAGTCAGAAAAG
GLAST	Reverse	CTTCTCCGTTGCTTTTGGTC
MCT-1	Forward	AGAAGCCAAAGGAGACGATG
MCT-1	Reverse	GATGGTTTTGGATGTCGTGG
MCT-4	Forward	TCTCTCCACAAATGGTGTGC
MCT-4	Reverse	CAAGGTGCCTGAGTCTTCCT
Cx43	Forward	TTCCTTTGACTTCAGCCTCC
Cx43	Reverse	CGTGGAGTAGGCTTGGAC
ApoE	Forward	CAATTGCGAAGATGAAGGCTC
ApoE	Reverse	TAATCCCAGAAGCGGTTCAG
VNUT	Forward	CTTCATTCTACTCTCCTGGCTG
VNUT	Reverse	CGGAGATGAACCCACTGAATAG
Stx4	Forward	CTAAAAGCCATAGAGCCCCAG
Stx4	Reverse	TCGGTATTCGGACTGCATTG
SNAP23	Forward	TCTAGAGTCCGAGAACTGTGG
SNAP23	Reverse	TGGGCACAGAAATACGGATAC
VAMP3	Forward	GCTGCCAAGTTGAAGAGAAAG
VAMP3	Reverse	TCGGGCTTCAGTTTCATCG
Munc18c	Forward	AAGAGTGGCCGTATTGTTCC
Munc18c	Reverse	TTAGTTCTGGGTTTCTGGCG
ITPR1	Forward	GATGCTAAAGAGGGACAGAAGG
ITPR1	Reverse	GCAGCGGAGAATGAGATCAAC
ITPR2	Forward	GAAGAGGGTAGCACATTACGG
ITPR2	Reverse	CTGAATCCTGTCCAGAGAAGC
ITPR3	Forward	AGGTCAACTCTGTCAACTGC
ITPR3	Reverse	CATCACAGGTCAGGAACTTCTC

Full unedited gel for Figure 4B

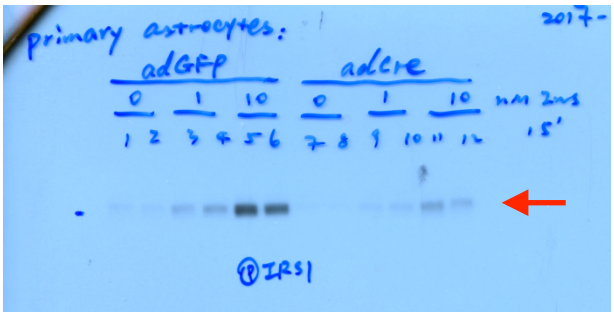

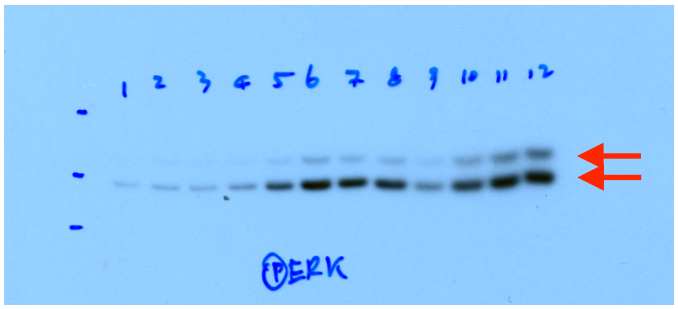

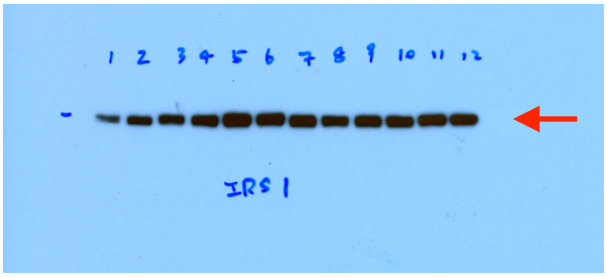

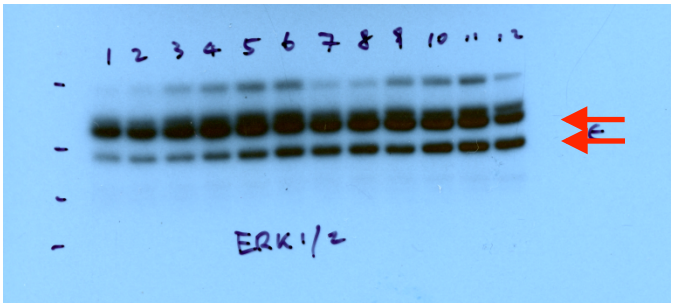

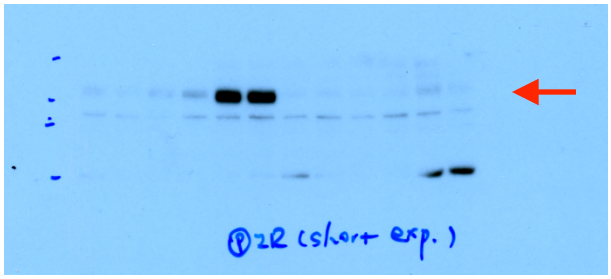

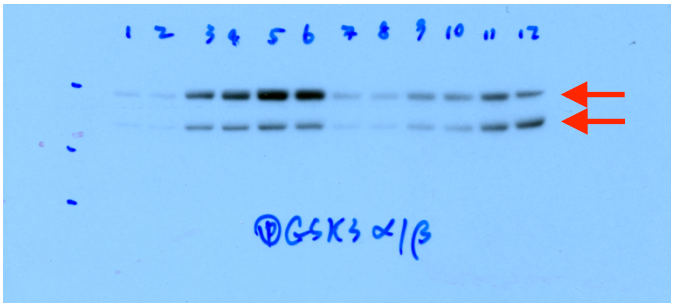

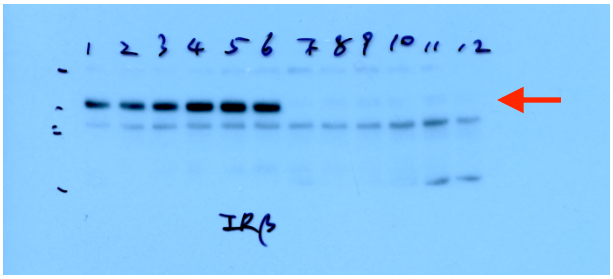

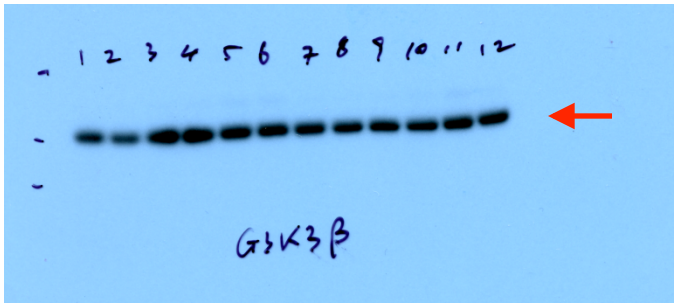

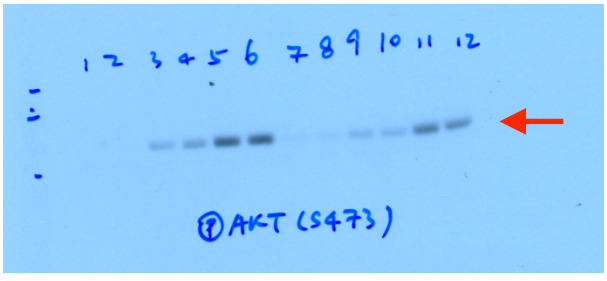

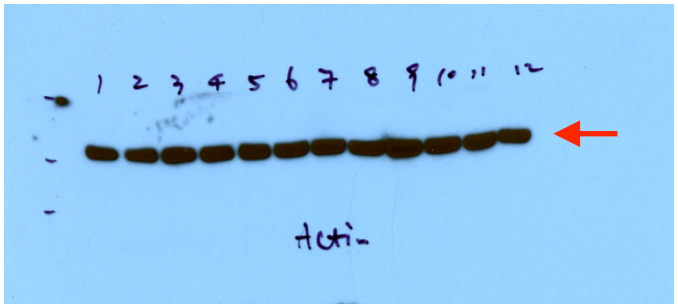

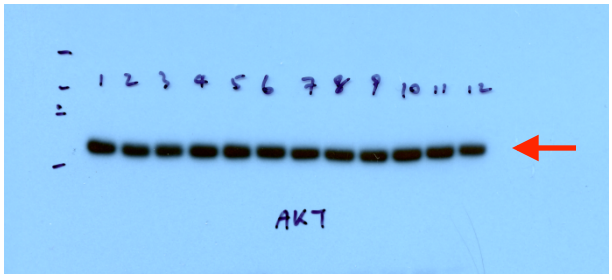

Full unedited gel for Figure 5A

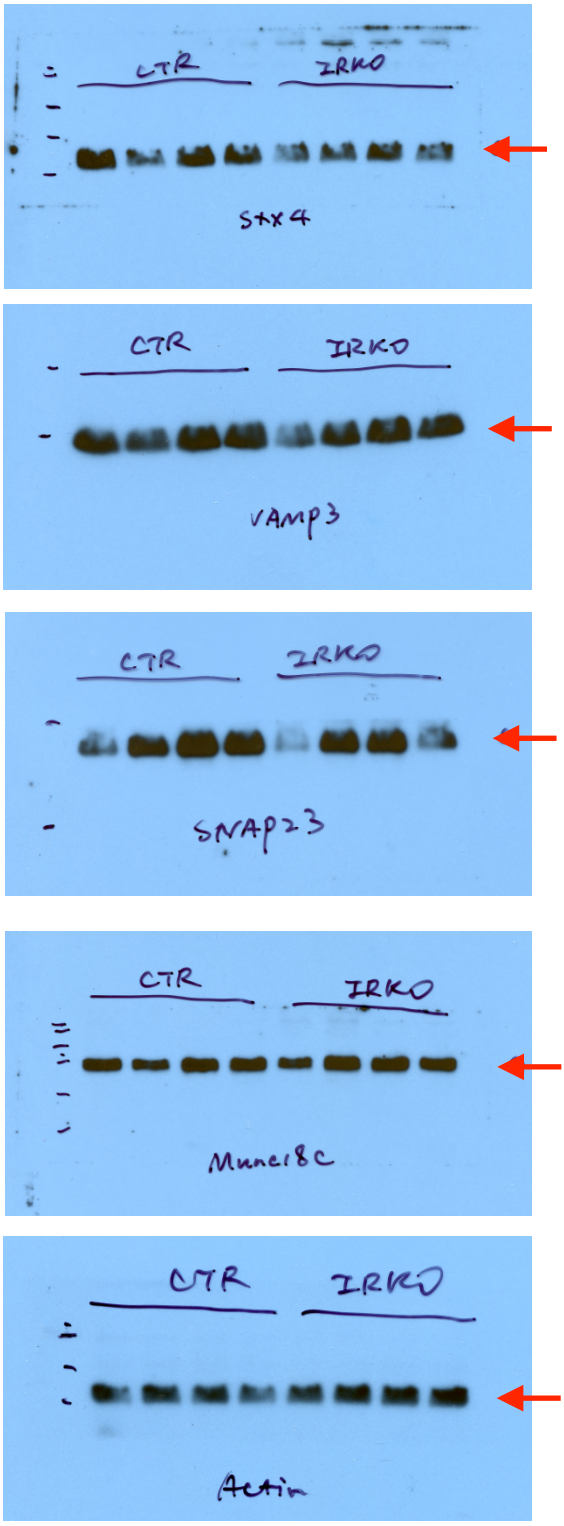

Full unedited gel for Figure 5B

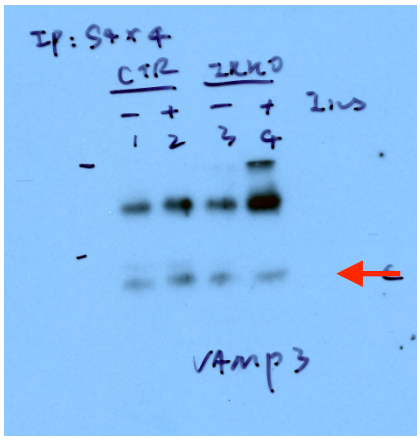

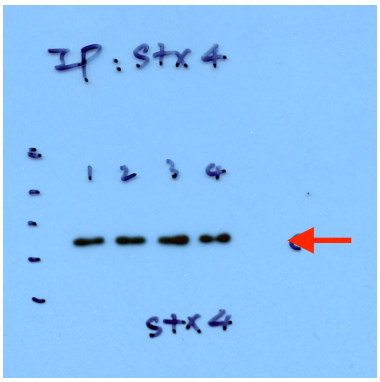

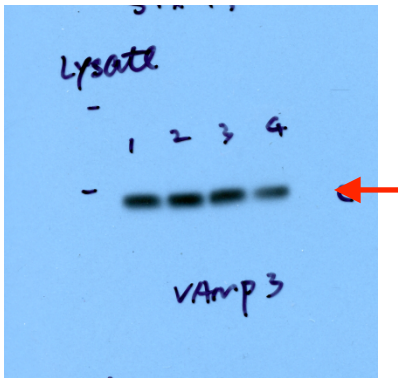

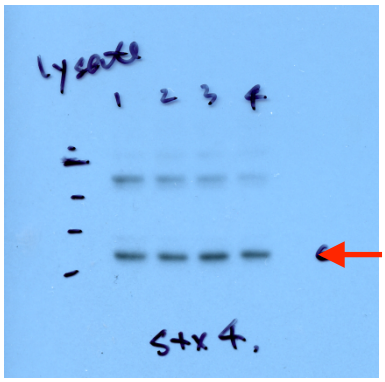

Full unedited gel for Figure 5C

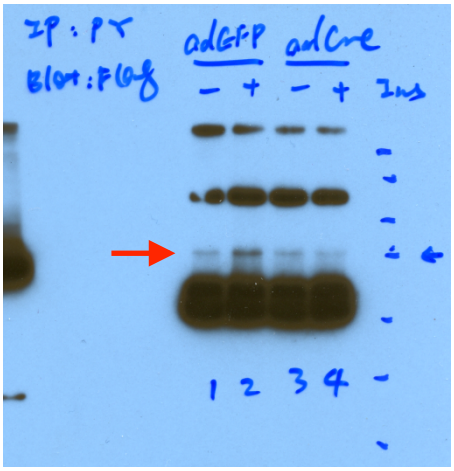

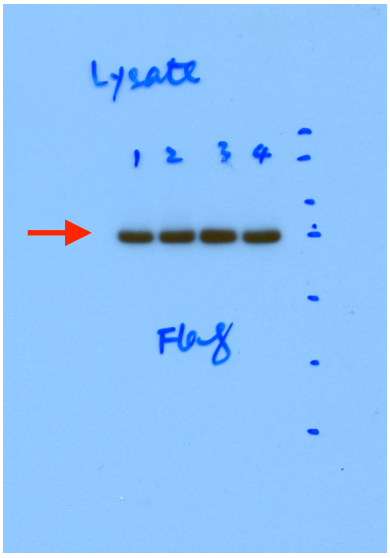

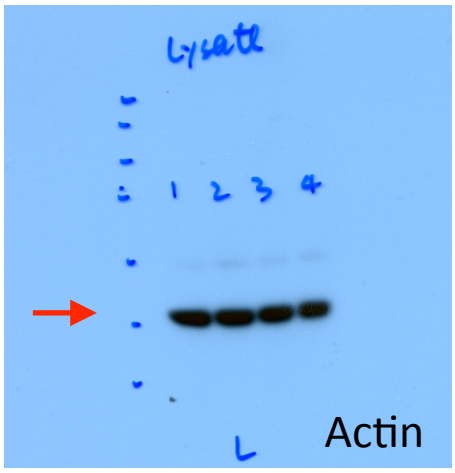

Full unedited gel for Supplemental Figure 1F

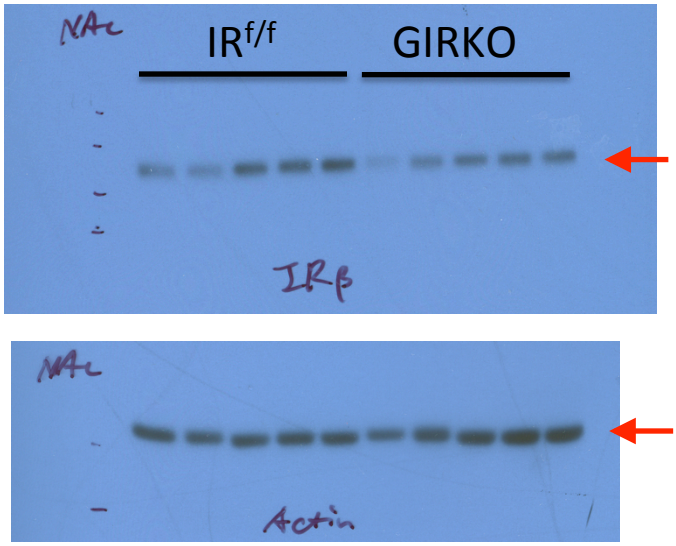

Full unedited gel for Supplemental Figure 13